

Linking wood density records of common beech (*Fagus sylvatica* L.) with temperature and precipitation variability from a temperate lowland site.

Jaime Bytebier^a, Tom De Mil^b, Margot Vanhellemont^c, Kris Verheyen^c, Kristof Haneca^d, Jan Van den Bulcke^{a,*,1}

^a UGCT – UGent-Woodlab, Laboratory of Wood Technology, Department of Environment, Ghent University, Coupure Links 653, 9000 Ghent, Belgium

^b Forest is Life, TERRA Teaching and Research Centre, Gembloux Agro Bio-Tech, University of Liège, Passage des Déportés 2, 5030 Gembloux, Belgium

^c Forest & Nature Lab, Department of Environment, Ghent University, Geraardsbergsesteenweg 267, 9090 Melle, Belgium

^d Flanders Heritage Agency, Havenlaan 88 box 5, 1000 Brussels, Belgium

ARTICLE INFO

Keywords:

Fagus sylvatica
Intra-annual wood density variations
Maximum latewood density
Radial growth
X-ray micro-Computed Tomography

ABSTRACT

European lowland beech stands are under pressure by current climate change and increased drought spells. Climate sensitivity of trees is most commonly studied by examining tree-ring width records and wood density-based time series, yet the potential of the latter is underexplored for hardwoods and beech (*Fagus sylvatica* L.) in particular. Here, we investigate how variability in radial growth, Maximum Latewood Density (MXD) and intra-annual wood density records in lowland beech are related to monthly and daily temperature (T) and precipitation (P) records, as well as the Standardized Precipitation Evapotranspiration Index (SPEI), during the past 50 years. 45 increment cores were collected from healthy (co-) dominant beech trees in Flanders (northern Belgium). We used X-ray micro-Computed Tomography (XμCT) to obtain wood density and tree-ring width series. By dividing every tree-ring into 4 sectors of equal radial width, we also assessed climatic forcings on intra-annual wood density variability (meanQi, i = 1:4). Water availability (SPEI) is the most important factor limiting radial growth, whereas MXD is correlated with summer temperature (period May–July, $r = 0.334$). Scanning resolution (110, 60, 20 μm) proves to be an important parameter when interpreting MXD values. We found that to quantify climate signals at the end of the growing season, density values should be representative for a relatively large part of the latewood. Our results also suggest that a sector approach is useful by showing climatic influences during the entire growing season. Wood density at the beginning of the growing season is mainly influenced by water availability (meanQ₁~SPEI, $r = 0.416$), whereas towards the end of the growing season only significant correlations with temperature were observed (meanQ₄~T, $r = 0.347$). We recommend to further explore MXD values for hardwood trees in lowland Europe.

1. Introduction

European forests, covering more than a third of Europe's land surface (FOREST EUROPE, 2020), are affected by climate change and shifts in tree species distributions, and severe economic consequences can be expected (Hanewinkel et al., 2013). European beech (*Fagus sylvatica* L.) is one of the most abundant and dominant tree species within these forests (del Río et al., 2017). The natural distribution area of beech covers a wide range of ecological and climatological zones, ranging from the southern part of Scandinavia, the temperate lowlands along the North Sea coast, down to the Mediterranean. Its distribution towards the

east is limited by the hot summers of the continental climate and extends to the Carpathians and the Balkan Mountains. Due to its important ecological and economic value, this deciduous tree has been very popular by forest managers, recreationists and eco-physiologists (Diaconu et al., 2016; Goossens, 2021). Climate change is putting this dominant position under pressure (Reyer et al., 2013; Allen et al., 2015). However, it remains difficult to assess where and how critical tree species are under pressure due to the changing climate (Mcdowell et al., 2008; Allen et al., 2015; Hartmann et al., 2018) and whether regional-scale stress will lead to a widespread mortality. Therefore, there is an urgent need to assess the impact of climate change on vegetation, associated

* Corresponding author.

E-mail address: Jan.VandenBulcke@UGent.be (J. Van den Bulcke).

¹ Present address: Coupure Links 653, 9000 Ghent, Belgium.

ecosystems and their feedback to the climate system (Scholze et al., 2006; Caillieret et al., 2019).

Forest vitality has been continuously monitored in Europe since the 1980 s, and the intensive monitoring plots of ICP Forests (<http://icp-forests.net/>) offer the opportunity to study the effects of air pollution and climate change on forest condition. Research by Sousa-Silva et al. (2018), using data from Belgian plots of ICP Forests, showed an increasing trend in crown defoliation for beech trees between 1990 and 2015. This upward trend was believed to be triggered by increasing drought stress. Increasing levels of defoliation are also observed in other European countries (Carnicer et al., 2011; Bussotti et al., 2018). Crown defoliation is the most commonly used indicator of tree vitality, however it is rather unspecific with respect to potential causes of damage, and possible links with tree functioning remains unclear. Therefore, it has been proposed to combine defoliation assessments with measurements of other tree vitality indicators (Gottardini et al., 2020). Cherubini et al. (2021) reported that tree-ring data can be used to enhance our understanding of tree vitality, in particular when using long tree-ring series.

The growth-ring pattern of living trees can be considered as archives of the past and biosensors of the present, as they offer a unique view on the trees response to fluctuating environmental conditions (Babst et al., 2017). Thus, the study of growth-ring patterns allows to accurately estimate growth rate and survival of tree species in the context of current climate change. While several studies have been performed on the impact of the environment on beech radial growth (i.e. tree-ring width), little is known about how variability of temperature and precipitation affects wood density (WD) and anatomical characteristics (Arnič et al., 2021). However, tree-ring width (TRW) may have a relative weak signal (site and climate region dependent) as ring widths are an integration over the entire growing season and only provide a single measurement for the entire growing season, during which environmental conditions can change dramatically (Van der Werf et al., 2007). Furthermore, especially in temperate, maritime climate zones with less extreme conditions (e.g. centrally in the geographical distribution range of a species, such as in many parts of Western Europe), the use of TRW is often inadvisable (Pritzkow et al., 2016), in contrast to peripheral populations at the edge of their distribution area (Dorado-Liñán et al., 2017). We must therefore look for more sensitive climate proxies in order to assess tree performance more accurately.

WD can be considered as an integrator of ecophysiological activity, which may provide novel and additional information on climate–growth relationships of trees compared to radial growth data (Bouriaud et al., 2004; van der Maaten et al., 2012). WD is determined by wood anatomical characteristics (e.g. cell wall thickness or size and density of sap transporting vessels), which in turn are shaped by prevailing environmental conditions, and hence steered by climatic variables (van der Maaten et al., 2012). Especially for conifer trees, relationships between maximum latewood density (MXD) and summer temperature have been established and are (widely) used for climate reconstructions (Schweingruber et al., 1978; Briffa et al., 1998; Björklund et al., 2017, 2019), even for periods that go back more than a thousand years in time (Esper et al., 2018; Klippel et al., 2019). St. George and Esper (2019) state that MXD is a superior climate-proxy compared to TRW in conifer trees.

The majority of these climate–growth relationships based on WD were established for conifer tree species. Due to the more complex wood anatomical structure of angiosperm species, such as beech, WD profiles are more complex to interpret and are therefore - up to now - rarely used for climate–growth analysis. However, densitometric studies on European beech showed that climatic signals are recorded in MXD and may provide valuable information related to the climate response of beech trees (Bouriaud et al., 2004; Skomarkova et al., 2006; Meinardus et al., 2012). Despite these findings, our knowledge of MXD and intra-annual WD variations in hardwoods and beech in particular, is still limited (van der Maaten et al., 2012; Bontemps et al., 2013).

WD is thus considered a valuable proxy in dendrochronology, yet

laborious wood sample preparation limits the widespread use for tree-ring analysis. There is an ongoing interest in developing new methods for studying WD in a more detailed and less time-consuming way, and less dependent on physical manipulations. A technique specifically reducing labour and time cost is X-ray micro-Computed Tomography (X μ CT). In contrast to classic X-ray densitometry or high-frequency densitometry, no physical surface treatment is necessary, and samples can be scanned immediately after drying (De Mil et al., 2016), or directly on sanded, mounted cores (De Mil et al., 2021). X μ CT is a non-destructive technique, complementary to existing techniques, enabling 3D tree-ring analyses to accurately and simultaneously study TRW and WD (Van den Bulcke et al., 2019).

The aim of this study was to quantify the relationship between climatic variables, TRW, and MXD for 45 beech trees in lowland Flanders (northern Belgium) for the past 50 years. We also studied the effect of X μ CT-scan resolution on MXD values, inspired by Björklund et al. (2019). Additionally, we divided each tree-ring into quarters (four sectors) to study climatic influences on the intra-annual WD profile. We hypothesize that (i) TRW and MXD are climate-sensitive tree-ring variables in beech, providing complementary information; (ii) X μ CT-resolution affects the strength of the climate association of MXD; and (iii) studying intra-annual WD variations can provide more knowledge about climatic influences on wood formation.

2. Material and methods

2.1. Study area

Samples were collected as part of the TREEWEEB project (https://treedivbelgium.ugent.be/pl_treeweeb.html) in lowland forests south of Ghent (50° 54' N 3° 35' E – 50° 59' N 3° 56' E). All sample plots are located in ancient forest fragments and are considered as mature forest stands of comparable age. The crown cover is at least 60% and obvious signs of recent forest management are absent in all plots. The climate in the study area is a temperate Atlantic maritime climate with an average annual temperature of 10.5 °C and average annual (fairly uniformly distributed) precipitation of 826 mm (1981–2010, Royal Meteorological Institute of Belgium).

2.2. Sample preparation and measurements

In August–September 2016, 45 cores were collected at selected sites in the framework of the TREEWEEB project. For each plot, at least two healthy (co-)dominant beech trees were sampled (minimum diameter 30 cm, minimum height 22.5 m). Two 5 mm increment cores were taken per tree, perpendicular to each other, at breast height (1.3–1.5 m) (Massart, 2017; Vanhellemont et al., 2019). All sampled trees had an age between 50 and 100 years. For this study, 45 cores from 22 beech trees were selected.

The samples were dried for 24 h at 103 \pm 1 °C and mounted in custom-made cardboard tubes and thereafter scanned with a resolution of 110 μ m (low resolution) using the X-ray micro-Computed Tomography (X μ CT) facility at UGent-Woodlab (www.woodlab.be), part of the BOF Centre of Expertise UGCT (UGent Center for X-ray Tomography, www.ugct.ugent.be) (Dierick et al., 2014). Reconstruction was performed with Octopus, a tomography reconstruction package for parallel, cone-beam and helical geometry as well as phase correction and retrieval (Vlassenbroeck et al., 2007). 12 cores of beech, out of the 45 cores scanned at 110 μ m, were rescanned at high resolution with X μ CT (20 μ m) to study the effect of resolution on MXD. A third resolution at 60 μ m, in between the other two, was obtained by artificially rescaling (downsampling) high resolution scan volumes via 'Mean 3D' tool in ImageJ (Fiji) software (Schneider et al., 2012).

In Fig. 1, X μ CT images and corresponding density profiles of the same tree-ring sequence scanned at 20 μ m (Fig. 1a) and 110 μ m (Fig. 1b) are shown.

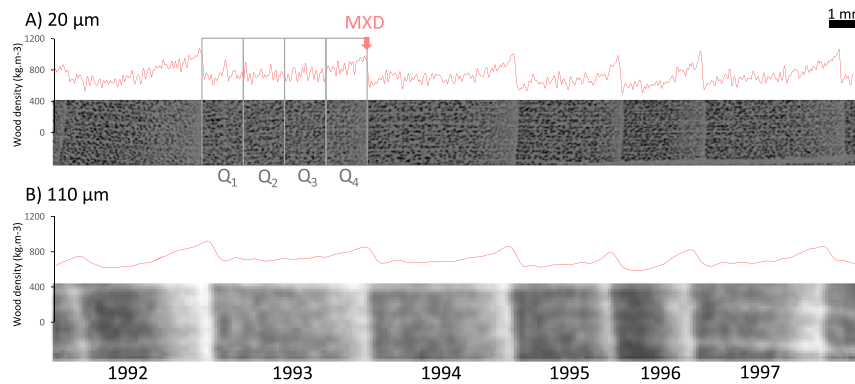


Fig. 1. Density profiles of the 1992–1997 tree-rings scanned at A) 20 μm and B) 110 μm . Maximum Latewood Density (MXD) in beech is defined as the density peak at the end of the growth ring. The quartile sector approach indicated with Q₁, Q₂, Q₃ and Q₄ is shown for one tree-ring (1993). In each sector the mean density is calculated.

2.3. Chronology construction and climate-growth analysis

X μ CT volumes were converted into TRW and MXD time-series, using custom-written software toolboxes (<https://dendrochronomics.ugent.be/#software>) (Van den Bulcke et al., 2014; De Mil et al., 2016). A chronology was built for every tree-ring characteristic and correlated to regional climate data for climate-growth analyses. Following chronologies were constructed: (1) TRW-110 μm and (2) MXD-110 μm , based on all samples, to compare the signal in both tree-ring variables; and (3) MXD-110 μm , (4) MXD-60 μm and (5) MXD-20 μm , based on the 12 samples that were rescanned at different resolutions, to study the effect of resolution on MXD. For 20 and 60 μm resolution there is no TRW-chronology, since scanning at 110 μm generates similar TRW values (Maes et al., 2017; Vannoppen et al., 2017).

Non-climatic trends were removed from each individual TRW and MXD-series with a 30-year cubic smoothing spline with 50% frequency cut-off, after truncating the first 30 years of each series to remove juvenile growth, using the 'detrend()' function of the dplR package (Bunn, 2008) in R (version 4.1.0, R Core Team, 2021). The TRW-chronology is composed only of those series passing EPS-based chronology stripping according to Fowler and Boswijk (2003), as implemented in the dplR package (Bunn, 2008). Climatic influences were tested with Pearson correlation coefficients in a climate-growth analysis using 'dcc()' function of the treeclim package (Zang and Biondi, 2015) and 'monthly_response()' function of the dendroTools R-package (Jevšenak and Levanič, 2018), during the period in which a robust common signal was captured: 1972–2016 for TRW ($n = 45$) and 1978–2016 for MXD ($n = 39$). These calculations were performed on monthly values from April of the year preceding growth, until September of the current growing season. We always focused on highly significant correlations that are stable in time and biologically interpretable (Jevšenak, 2020). We also assessed the stability of the response using different temporal windows and multiple detrending-methods, to verify that results are not biased due to a changing analysis method. In this study, however, we only show results for the abovementioned temporal window (1972–2016 for TRW and 1978–2016 for MXD) and detrending with a 30-year cubic smoothing spline with 50% frequency cut-off. Precipitation (P) and temperature (T) data (period 1972–2016) were sourced from the KNMI Climate Explorer (station code 6447, Uccle Belgium: 50° 48' N, 4° 20' E) (Trouet and Van Oldenborgh, 2013). In addition we used the Standardized Precipitation Evapotranspiration Index (SPEI) as an integrative measure of drought intensity (Vicente-Serrano et al., 2010). We calculated the SPEI for different timescales (3–24 months) for every month in the year from 1972 to 2016 (Beguería et al., 2017). The 15-month SPEI showed the highest correlation with tree-ring chronologies and was used in further analyses.

We also explored multi-month responses of T and P by aggregating

monthly values in order to maximize correlation with TRW and MXD-chronologies and the response on a fixed window of consecutive. The latter analysis was performed with a fixed period from April–August for TRW, as ring widths are an integration over the entire current growing season and the period May–July for MXD, as maximum density is related to the last formed latewood (end of growing season), and consequently the link with climate variables in the summer months is most likely (Čufar et al., 2008; Michelot et al., 2012; Lehnbach et al., 2021). In addition to working with monthly data, we analyzed the influence of daily climate data using the dendroTools R-package (Jevšenak and Levanič, 2018), more specifically the 'daily_response()' function, to provide more detailed analyses of climate-growth relationships (Jevšenak, 2020). In this study we used daily climate data from the Uccle weather station to in-depth analyze the effect of resolution on MXD.

2.4. Sector approach

To improve the level of detail of WD associations with T, P and SPEI at the intra-annual scale, we divided each tree-ring into 4 consecutive sectors (quantiles) of equal radial width from earlywood (Q1) to latewood (Q4) (Puchi et al., 2020). For each sector, the mean density was computed. For this purpose, a dedicated MATLAB function was written and added to the CoreComparison toolbox (De Mil et al., 2016). We performed this sector approach only on the 20 μm X μ CT volumes. Maximum density of the last sector (maxQ₄) was also calculated, and equals MXD at 20 μm . All 5 series for each core (mean density per sector: meanQ_i with $i = 1, 2, 3$ or 4 and maxQ₄) were truncated the first 30 years to remove juvenile growth, then detrended with a 30-year cubic smoothing spline with 50% frequency cut-off and thereafter averaged to build chronologies using respectively the 'detrend()' and 'chron()' function of the dplR package from Bunn (2008). Both daily and monthly climate data were used to quantify climate-growth relationships at sector level, using treeClim and dendroTools (Jevšenak and Levanič, 2018; Zang and Biondi, 2015).

3. Results

3.1. Comparison of climatic signal MXD vs. TRW

Climate-growth correlations, using the detrended TRW- and MXD-chronology (Fig. 2) at 110 μm , are presented in Fig. 3. Radial growth of beech is negatively correlated with T in June, July and August of the preceding year (August showing a significant correlation: $p < 0.05$). Temperature in current June, July and August also seems to negatively affect TRW ($p > 0.05$). Spring T (current March, April and May) on the other hand, positively affects TRW ($p > 0.05$). Monthly P is almost always positively correlated with ring width, with significant correlations

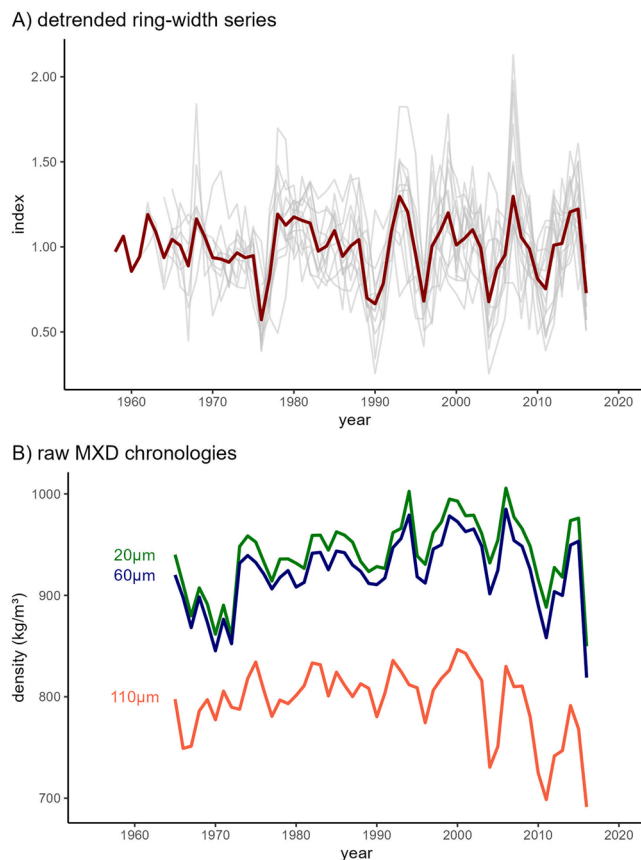


Fig. 2. A) Detrended and indexed ring-width chronology (1958–2016). Only the series that passed EPS-based stripping after Fowler and Boswijk (2003) were included in the chronology ($n = 15$). The underlying individual tree-ring series have ring-widths ranging between 0.4 mm up to 7 mm wide (mean 2.9 ± 1.1 mm). B) Raw MXD chronologies (1965–2016) for the three scanning resolutions ($n = 12$).

($p < 0.05$) in previous June, December and current May (Fig. 3a). MXD of beech is positively correlated with T in current May, June and July, with the latter being significant ($p < 0.05$). No significant effects ($p > 0.05$) of P on MXD were observed (Fig. 3b).

In a next step monthly T and P data was grouped and a 15-month SPEI was computed, since it is more likely that tree-ring characteristics are shaped by accumulated climatic conditions over several months. The highest correlations between tree-ring characteristics (TRW, MXD) and aggregated climatic variables are found for TRW, in particular effects of P and water availability (quantified as 15-month SPEI) on beech radial growth. A significant positive influence of P during the previous growing season (i.e. previous April until August) ($\text{TRW} \sim \text{P}$, $r = 0.580$, $p < 0.05$, $n = 45$) and water availability in current May until July ($\text{TRW} \sim \text{SPEI}$, $r = 0.570$, $p < 0.05$, $n = 45$) is observed. Temperature in previous summer (i.e. previous June until August) has a negative correlation with TRW ($\text{TRW} \sim \text{T}$, $r = -0.423$, $p < 0.05$, $n = 45$). No significant effect of P (in current March until May) and water availability (in current April until June) are found on MXD ($\text{MXD} \sim \text{P}$, $r = 0.264$, $p > 0.05$, $n = 39$; $\text{MXD} \sim \text{SPEI}$, $r = 0.303$, $p > 0.05$, $n = 39$). The highest correlation of MXD is with T in the period May until July ($\text{MXD} \sim \text{T}$, $r = 0.334$, $p < 0.05$, $n = 39$). Temperature is the only climatic variable that has a significant correlation with MXD.

We complement the previous approach with an analysis that focuses on groups of consecutive months that most likely have an influence on a tree-ring characteristic, i.e. April until August for TRW and May until July for MXD (both periods in the current year). This fixed window analysis is visualized in Fig. 3c. During the period May until July, T is the

only climatic variable having a significant correlation with MXD ($\text{MXD} \sim \text{T}$, $r = 0.334$, $p < 0.05$, $n = 39$). No significant effect of P and water availability is observed ($\text{MXD} \sim \text{P}$, $r = 0.016$, $p > 0.05$, $n = 39$; $\text{MXD} \sim \text{SPEI}$, $r = 0.264$, $p > 0.05$, $n = 39$). The radial growth of beech is significantly correlated with water availability during the growing season (April until August) ($\text{TRW} \sim \text{SPEI}$, $r = 0.556$, $p < 0.05$, $n = 45$). No significant effect of P and T is observed during the same period ($\text{TRW} \sim \text{P}$, $r = 0.253$, $p > 0.05$, $n = 45$; $\text{TRW} \sim \text{T}$, $r = -0.028$, $p > 0.05$, $n = 45$).

3.2. Effect of resolution on MXD

To study the effect of X μ CT-scan resolution on MXD, we focused on the correlation between MXD and T during the period May until July (of current year), as T is the only variable having a significant correlation with MXD. At all three resolutions (scanned 20 and 110 μm , rescaled 60 μm), the highest influence of T is related to the period May–July.

Differences are observed in mean MXD-value between the different resolutions: higher MXD-values are obtained at 20 μm , compared to 110 μm (940.35 vs. 792.87 kg/m^3) (Fig. 2b). Climate-growth correlations are presented in Fig. 4. The highest correlation between MXD and T is found at low resolution ($\text{MXD} \sim \text{T}$ 110 μm , $r = 0.405$, $p < 0.05$, $n = 39$). The MXD-chronology at 20 μm shows the least pronounced correlation with T ($\text{MXD} \sim \text{T}$ 20 μm , $r = 0.301$, $p < 0.05$, $n = 39$). The intermediate resolution of 60 μm , has a correlation coefficient in between ($\text{MXD} \sim \text{T}$ 60 μm , $r = 0.334$, $p < 0.05$, $n = 39$).

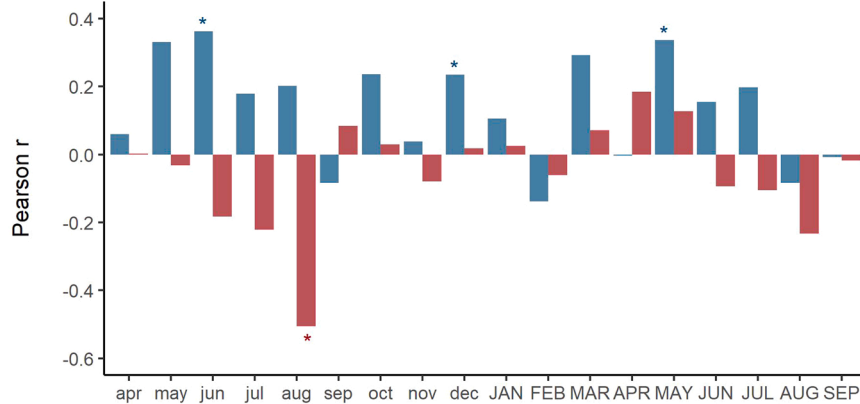
To study the effect of resolution more in detail, we also used daily data. Instead of grouping months, dendroTools ‘daily_response()’ function groups consecutive days, and thus allows to analyze differences, at daily basis, between different X μ CT-scan resolutions. We opted to group at least 21 days (Jevšenak and Levanič, 2018). Analyses with daily data confirm the significant influence of T during the period May–July (Fig. 5a,b). At 110 μm , the highest correlation between MXD and daily T is found during the period 4 May until 24 May ($\text{MXD} \sim \text{daily T}$ 110 μm , $r = 0.435$, $p < 0.05$, $n = 39$). Thus, monthly data allow to determine which months (groups of consecutive months) have a significant correlation with a tree-ring characteristic, and daily data make it possible to determine which days within this period have the largest influence. MXD-values at 110 μm are consequently significantly correlated with T from May until July, with the highest correlation in May (4 May – 24 May) (Fig. 5b).

At 20 μm , the highest correlation between MXD and daily T is found for the period 24 April until 20 May ($\text{MXD} \sim \text{daily T}$ 20 μm , $r = 0.336$, $p < 0.05$, $n = 39$). Significant correlations are also observed with daily T later in the growing season (i.e. for wider windows starting in May). Thus, MXD-values at 20 μm are significantly correlated with T during the period May–July, with the highest correlation from 24 April until 20 May (Fig. 5a). However, these correlations are less pronounced compared to low resolution scans, for both monthly (Fig. 4) and daily T data (Fig. 5).

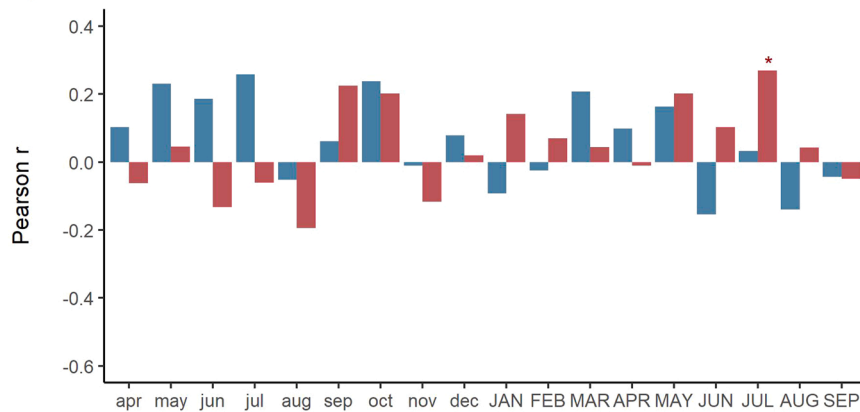
3.3. Sector approach

For each of the four sectors (quantiles Q₁:Q₄) a chronology was built representing the mean density (Fig. 6). The mean density of sector 4 (meanQ₄), the last formed quarter of a tree-ring, is significantly positive correlated with T from May until July (meanQ₄~T, $r = 0.347$, $p < 0.05$, $n = 39$). Daily T data confirms the significant correlation with T in May–July, with the highest correlation from 3 May until 15 June (meanQ₄~daily T, $r = 0.422$, $p < 0.05$, $n = 39$). No significant effect of P and water availability (quantified as 15-month SPEI) on meanQ₄ is observed (Table 1). The maximum density of sector 4 (maxQ₄) equals the MXD-value (MXD at 20 μm , since 20 μm X μ CT volumes are used in sector approach), as exactly the same density values and climate-response is observed. This confirms that MXD is related to the last formed latewood, and is therefore by no means an intra-annual WD fluctuation. MaxQ₄ is significantly positive correlated with T in May–July

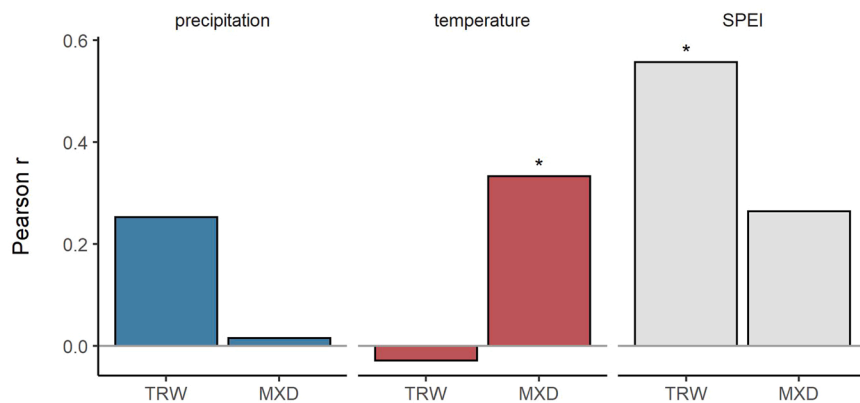
A) TRW



B) MXD



C) Fixed window



(maxQ₄~T = MXD~T 20 μ m, $r = 0.301$, $p < 0.05$, $n = 39$) (Table 1).

MeanQ₃ is significantly positive correlated with T during the period May-June (meanQ₃~T, $r = 0.371$, $p < 0.05$, $n = 39$). No significant effect of T in July is observed, with monthly and daily T data, in contrary to sector 4. Precipitation and water availability have no significant correlation with meanQ₃ (Table 1).

Both T, P and SPEI have a significant correlation with meanQ₂. Temperature is significantly correlated with meanQ₂ during the period May-June (meanQ₂~T, $r = 0.338$, $p < 0.05$, $n = 39$), P and meanQ₂ during the period March-April (meanQ₂~P, $r = 0.334$, $p < 0.05$, $n = 39$). The most pronounced (positive) influence on mean density of Q₂ is related to water availability in April-May (meanQ₂~SPEI,

$r = 0.401$, $p < 0.05$, $n = 39$).

The mean density of sector 1 (meanQ₁), the first formed quarter of a tree-ring, is significantly correlated with T (period May-June), P (March-April) and SPEI. The highest (positive) correlation is with water availability during the period April-May (meanQ₁~SPEI, $r = 0.416$, $p < 0.05$, $n = 39$) (Table 1). In terms of monthly groupings, there are no clear differences between meanQ₁ and meanQ₂ (Table 1). However daily P data indicates a difference: meanQ₂ is highly influenced by P in March-April, and to some extent to P at the beginning of May. MeanQ₁, however, only shows high correlations with daily P data in March and April. No clear relation to P in early May is observed for meanQ₁.

Fig. 3. Climate-growth correlations for TRW and MXD at 110 μ m, with monthly mean temperature (T) in red and total monthly precipitation (P) in blue. A) Pearson correlation of TRW-chronology with monthly data of T and P, for the period 1972–2016. B) Correlation of MXD-chronology with monthly data of T and P, for the period 1978–2016. Current growing season months are capitalized. C) Groups of consecutive months in fixed window analysis. Pearson r quantifies the correlation between P, T and SPEI (grey) and the tree-ring data during the fixed period April-August for TRW (left bar), and May-July for MXD (right bar) (fixed periods of current year). Stars denote significant correlations ($p < 0.05$).

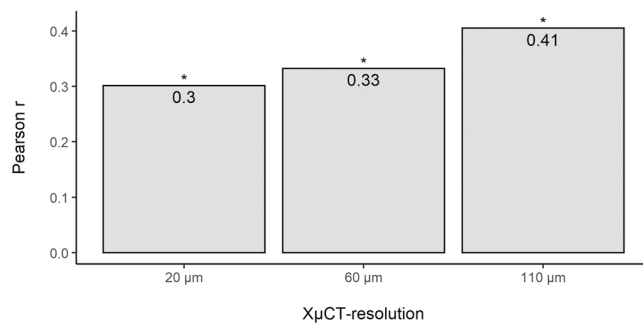


Fig. 4. Effect of X μ CT-resolution on MXD ~ T relationship (period May-July; 1978–2016). Asterisks denote significant correlations ($p < 0.05$).

4. Discussion

4.1. MXD is a climate-sensitive tree-ring variable in beech

Tree-ring widths are influenced by the length of the growing season

and the rate of cell production in the cambium, both driven by environmental and climatological conditions (Prislan et al., 2013). Radial growth of beech is negatively influenced by summer temperature, especially during previous summer (Fig. 3a), and highly positively influenced by precipitation in the previous growing season (to a lesser extent during current growing season) and water availability during late spring-early summer (Fig. 3a,c). The negative correlation of TRW with temperature in the previous summer months indicates that high evapotranspiration rates and reduced photosynthesis could reduce the amount of stored carbohydrate reserves (Van Der Werf et al., 2007). This implies that stored carbohydrates from the previous year affect growth in the current year, which appears to be characteristic of deciduous trees (Kozłowski and Pallardy, 1997). Strong positive correlations with precipitation and water availability demonstrate a high drought susceptibility of beech radial growth (Van Der Werf et al., 2007; Giagli et al., 2016; Meyer et al., 2020). Beech is sensitive to drought throughout the growing season, and especially to early summer droughts (Dittmar et al., 2003; Lebourgeois et al., 2005; Debel et al., 2021).

Unlike TRW, climatic conditions of mainly the current year influence MXD and therefore a slightly lower autocorrelation (i.e. reduced

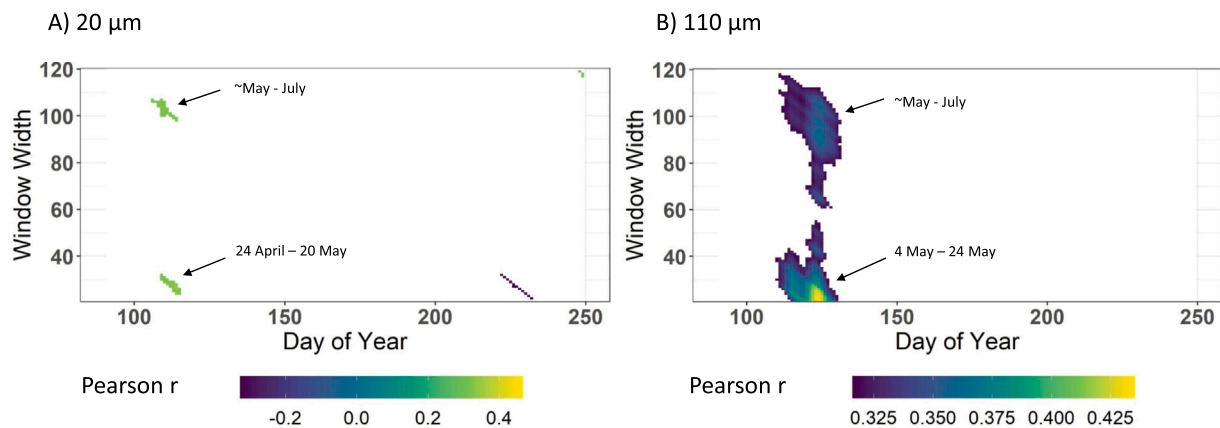


Fig. 5. Output of the DendroTools daily response analysis for MXD and mean temperature (T) at A) 20 μ m and B) 110 μ m during the period 1978–2016. Day of year reference (DOY, x-axis) is the starting moment of each calculation, ranging from beginning of April (DOY c. 100) until beginning of September (DOY c. 250), with a certain window width (y-axis). Only significant correlations ($p < 0.05$) are displayed.

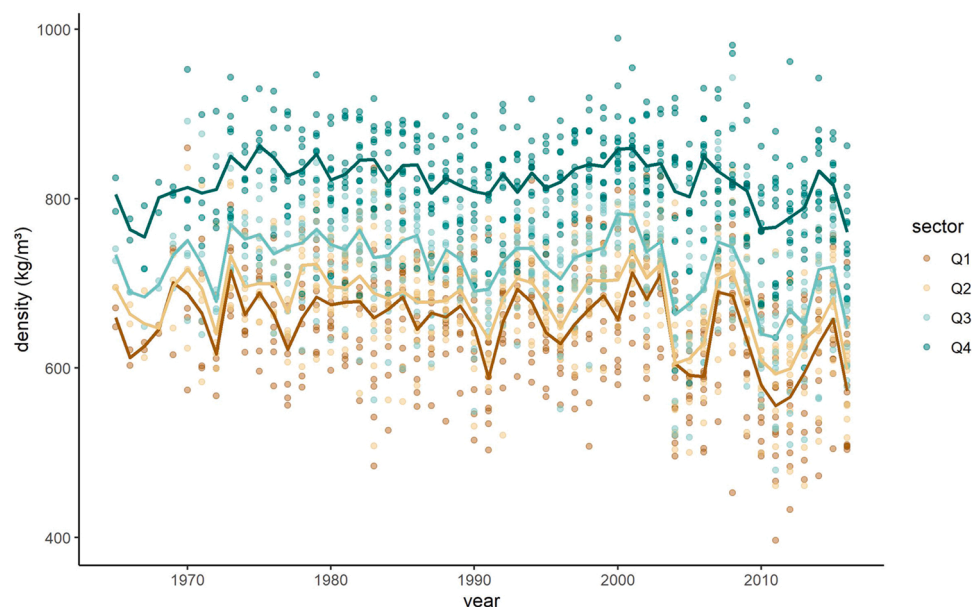


Fig. 6. Chronologies of mean density values for each of the four sectors (quantiles) of each growth ring ($n = 12$).

Table 1

Climate-growth correlations (1978–2016) in the different sectors. Pearson correlation coefficients are used to quantify the relationship between meanQ_i (i = 1:4), maxQ₄ and monthly grouped data of temperature, precipitation or SPEI (from current year). Asterisks denote significant (p < 0.05) correlations. Grey boxes show the highest correlation per column).

	meanQ ₁	meanQ ₂	meanQ ₃	meanQ ₄	maxQ ₄
Temperature	May-June 0.335 *	May-June 0.338 *	May-June 0.371 *	May-July 0.347 *	May-July 0.301 *
Precipitation	March-April 0.270 *	March-April 0.334 *	March-May 0.340	March-May 0.262	March-May 0.194
SPEI	April-May 0.416 *	April-May 0.401 *	April-May 0.317	March-May 0.091	May-July 0.148

influence of the previous year's climate) is observed (average AC1: 0.562 for TRW and 0.496 for MXD). This corresponds to the findings of Skomarkova et al. (2006), where lower autocorrelations were also observed in MXD-series for beech. Lower autocorrelations for a tree-ring characteristic compared to TRW-series could offer some practical advantages over ring widths (Davies and Loader, 2020). Temperature, during the period May until July, is the only climatic variable having a significant correlation with MXD (Fig. 3b,c). Skomarkova et al. (2006) and Meinardus et al. (2012) found positive correlations between MXD and temperature during the second half of the growing season in beech trees as well. Z'Graggen (1992) showed that MXD in beech towards the end of the growing season is mostly explained by climate. Thus, MXD is mainly influenced by current growing season conditions, especially by summer temperature, suggesting that MXD is a promising record to further examine in beech trees.

4.2. X_μCT-resolution affects the strength of the climate association with MXD

To study the effect of X_μCT resolution on MXD-related analyses, we quantified both the effect on the absolute MXD-values and the strength of the climate association. At 20 μm, the mean MXD-value is clearly larger than the mean MXD-value at 110 μm (940.35 vs. 792.87 kg/m³). Thus, scanning exactly the same tree-ring but at another resolution, results in a different MXD-value, which applies to both small and wide rings. This can be explained because MXD-values at different resolutions reflect maximum densities integrated over a larger (low resolution) or more limited (high resolution) part of the tree ring (Jacquin et al., 2017).

In Fig. 4, we quantified the strength of the MXD ~ T (period May-July) relationship for different X_μCT resolutions (20, 60 and 110 μm). At all three resolutions, this relationship is significant, but the effect of temperature is most pronounced when based on low-resolution scans. Daily temperature data also show that the strongest climate association of MXD is observed at low resolution (Fig. 5a,b). However, the opposite effect is observed in conifer trees (Björklund et al., 2019). To accurately capture MXD in conifer trees, commonly done at temperature-limited sites (Alpine or boreal climates), high measurement resolution is essential, as the MXD-variable may be a function of a few latewood cells within an annual ring (Vaganov et al., 2006). Then, especially for narrow tree rings, a low scanning resolution might lead to a weaker relationship between MXD and summer temperature due to a systematic underestimation (bias) of MXD (Björklund et al., 2019).

Because little research has been done on MXD in hardwoods and diffuse-porous species in particular (van der Maaten et al., 2012; Bontemps et al., 2013), it is not known whether high-resolution scans for beech are also required or informative. Fig. 4 indicates that a high X_μCT resolution is not necessarily essential when trying to quantify and optimize the climate-growth relationship. We hypothesize that due to the longer growing season, and hence wider rings, for beech trees in lowland Flanders, compared to conifers in boreal or Alpine climates,

MXD at high resolution, representing a small part of the latewood, does not capture the climatic signal properly, compared to MXD at lower resolution, which is representative for a larger part of the latewood (for further discussion we refer to the next section).

We observe that the Rbar of MXD is higher for 110 μm than for 60 μm, which is on its turn higher than the one at 20 μm. We have also tested the approach as explained in Björklund et al. (2019) by taking the highest value pixels (e.g. fibres-only) and then the climate signal disappears for the 20 μm resolution. Both observations hint at the importance of vessels in the MXD signal: at 20 μm the MXD value is really at the end of the tree ring, where hardly any vessels are present. Of course, more work is needed to fully unravel the MXD signal (see further). Therefore, the 110 μm approach (Fig. 4) shows the highest correlation, whereas for the 20 μm a possible explanation would be that only fibres are measured, which have a limited effect on the density profile (Peters et al., 2020). More detailed investigations on the anatomy-density relationship are needed, and one possible opportunity is the use of higher-resolution scans (Van den Bulcke et al., 2019).

Our results thus clearly show that X_μCT resolution affects the strength of the climate association of MXD. The highest temperature-sensitivity is in fact observed at MXD-values derived from the X_μCT scans with the lowest resolution of 110 μm. This is further confirmed in Fig. 5, where daily temperature data are used, that generated a smaller area of significant correlations for the 20 μm data (Fig. 5a).

4.3. Studying intra-annual wood density variations can reveal climatic influences on wood formation

Analysis of WD has developed into a valuable dendroecological tool for studying the relationship between WD and TRW, cambial age, different environmental factors or silvicultural practices, especially for conifer species (Diaconu et al., 2016). WD variations of diffuse-porous tree species have rarely been analyzed (Bontemps et al., 2013; Bouriaud et al., 2004; Skomarkova et al., 2006; Zhang, 1995). We studied intra-annual WD variations in beech trees, by dividing every tree-ring into 4 equal sectors, to try to better understand climatic forcings on wood formation.

Previous studies showed that local environmental conditions play a key-role on WD variability in beech trees. Although Bouriaud et al. (2004) did not find an effect of soil water deficit on mean annual WD, a strong temperature influence on WD was observed during the last part of the growing season, corresponding to the latewood, where MXD is recorded. Bouriaud et al. (2004) concluded that WD variations of diffuse-porous trees are a response on climatic fluctuations similar as in conifer trees, however the magnitude of the response is far weaker. Similarly, Z'Graggen (1992), Skomarkova et al. (2006) and Meinardus et al. (2012) found that MXD in beech is mostly explained by climate. Skomarkova et al. (2006) and Peters et al. (2020) also reported that WD variations in beech are mainly determined by variations in vessel properties and not by fibre properties. WD is positively related to water stress through the direct effect of cell turgor as well as by changes in hormonal balances and carbohydrate reserves (van der Maaten et al., 2012). van der Maaten et al. (2012) studied intra-annual WD variations in beech trees, and also illustrated that climatic forcings can be found during a major part of the growing season, thus not only restricted to the latewood. Diaconu et al. (2016) stressed the impact of water stress on wood formation as well. However, a lower mean annual WD was obtained at drier sites, even though the difference with moist sites is small, indicating an opposite effect as the one reported by van der Maaten et al. (2012). Lower WD on dry sites could be explained because earlywood vessels are grouped in more and larger clusters in narrow rings compared to moist sites with larger rings, which may indicate a higher vessel area within a single tree-ring on dry sites and consequently a lower WD (von Arx et al., 2013, 2020). This explanation directly links to the resolution discussion in the previous section. Due to 'scattering' of the vessels, MXD values might be more variable. Peters et al. (2020)

showed the limited impact of fibres on WD. Here, when looking at the different tree-ring sectors - Q1, Q2, Q3, Q4, we observe that the mean density value of each sector (Fig. 6) is related to a decreasing vessel area and/or grouping (cf. Miranda et al., 2022; Peters et al., 2020) and thus a decrease in size and number of vessels and an increase in fibre proportion towards the tree ring boundary. Fibre wall variation and vessel area/grouping were not measured in this study but further studies to disentangle the density profile are needed.

We found that in each of the 4 intra-annual ring sectors, WD is significantly affected by climatic conditions (Table 1). This implies that wood formation throughout the entire growing season is influenced by external factors. The influence of T, P and/or SPEI, however, is not a constant factor nor stable throughout the growing season. WD in the first two sectors is mainly driven by water availability in April-May. The more water is available during this period, the higher meanQ₁ and meanQ₂. However, in the last two sectors temperature - during the period May-June and May-July respectively for third and last sector - becomes the dominant environmental factor. The influence of P and SPEI on WD fades, and temperature is the only variable having a significant correlation with meanQ₃, meanQ₄ and maxQ₄ (Table 1). Thus, water availability mainly affects WD in the beginning of the growing season, while the effect of temperature increases towards the end of the growing season. Daily climate data (daily T and P) is an added value in determining the periods with the highest influence. It showed that meanQ₁ is mainly influenced by precipitation in March and April, whereas meanQ₂ also seems to be affected by precipitation in beginning of May. This is another indication that the earlier wood is formed, the more it is affected by conditions early in the growing season. Daily data also confirmed that July temperatures only seem to affect WD in the last sector.

Besides using scan resolution as a proxy for the integration zone in the latewood (Figs. 4 & 5), we also opted to directly vary the integration zone to determine WD. This was accomplished by constructing a chronology for maxQ₄ and meanQ₄ in the last sector (Table 1). MaxQ₄ is determined by the pixel with the highest density and is equal to MXD at 20 µm, whereas meanQ₄ is an integration over the entire last sector (Fig. 1a). For conifer trees, we would expect higher correlations between maxQ₄ (MXD) and temperature, compared to meanQ₄, as the MXD-variable can be a function of a few latewood cells within an annual ring (Vaganov et al., 2006). In this study we observed the opposite, as the correlation between meanQ₄ and temperature is the largest (Table 1). To maximize the climatic signals in latewood density for beech trees included in this study, it seems that scanning at high resolution, or thus integrating over a relative small part of the latewood, is not essential. The highest correlations are observed when low resolution XµCT scans (110 µm) are used, or when density values are integrated over a quarter of a tree-ring (which is in this study about 750 µm wide on average, with a range between 100 and 1750 µm). Due to a relative long growing season for beech trees in our lowland site (Lehnebach et al., 2021), it seems that a relative large part of the latewood needs to be taken into account to properly assess climate signals at the end of the growing season. However, we do not recommend to integrate density values over more than a quarter of a tree-ring, as meanQ₄ shows a lower temperature-sensitivity compared to MXD at 110 µm ($r = 0.347$ vs. $r = 0.405$, Fig. 4 & Table 1).

Exploring intra-annual WD variations of lowland beech in Flanders by means of XµCT has added value in quantifying climatic influences on wood formation. Water availability mainly drives wood formation at the beginning of the growing season, whereas towards the end of the growing season only temperature effects are observed. To maximize the correlation with temperature at the end of the growing season, integrating densities over a relatively wide part of the latewood seems to be recommendable, yet further research is needed to relate WD variations to the vessels, preferably for longer time-series and/or under contrasting climatic conditions.

5. Conclusions

Here, we showed that climatic variables have a significant influence on wood formation (WD and TRW) in lowland beech, as observed by XµCT. Despite short tree-ring series and a long growing season in a temperate maritime climate zone, clear effects of water availability were observed on radial growth. Our findings also bring new evidence regarding environmental drivers of WD. A sector approach shows changing climatic forcing on intra-annual WD throughout the growing season: from a precipitation driven response in the early sectors to a more temperature sensitive response in the last sectors of the growth rings. This opens new perspectives for future research on MXD and intra-annual WD variations in beech trees, or other diffuse-porous hardwoods, in Western-Europe. We consider this to be essential because, despite the promising results from this study, more research is needed concerning climatic forcings on WD and linked anatomical characteristics.

Declaration of Competing Interest

The authors declare that they have no known competing financial interests or personal relationships that could have appeared to influence the work reported in this paper.

Data availability

Data will be made available on request

Acknowledgements

Financial support for this research was provided via the UGent-GOA project 'Scaling up Functional Biodiversity Research: from Individuals to Landscapes and Back (TREEWEB)'. We are indebted to Stijn Willen for meticulous preparation of sample holders and samples and Ivan Josipovic for supporting the scanning process. We also acknowledge the BOF Special Research Fund for the support of the UGCT Center of Expertise (BOF.EXP.2017.0007) and of Jan Van den Bulcke (BOF Starting Grant, BOFSTG2018000701). This work was also supported by the Research Foundation – Flanders (FWO) through the project grant ACTREAL (G019521N).

References

- Allen, C.D., Breshears, D.D., McDowell, N.G., 2015. On underestimation of global vulnerability to tree mortality and forest die-off from hotter drought in the Anthropocene. *Ecosphere* 6. <https://doi.org/10.1890/es15-00203.1>.
- Arnič, D., Gričar, J., Jevšenak, J., Božič, G., von Arx, G., Prislan, P., 2021. Different wood anatomical and growth responses in European beech (*Fagus sylvatica* L.) at three forest sites in Slovenia. *Front. Plant Sci.* 12. <https://doi.org/10.3389/fpls.2021.669229>.
- Babst, F., Poulter, B., Bodesheim, P., Mahecha, M.D., Frank, D.C., 2017. Improved tree-ring archives will support earth-system science. *Nat. Ecol. Evol.* 1. <https://doi.org/10.1038/s41559-016-0008>.
- Beguería, S., Vicente-Serrano, S.M., and Beguería, M.S., 2017, Package 'SPEI'.
- Björklund, J., Seftigen, K., Schweingruber, F., Fonti, P., von Arx, G., Bryukhanova, M.V., Cuny, H.E., Carrer, M., Castagneri, D., Frank, D.C., 2017. Cell size and wall dimensions drive distinct variability of earlywood and latewood density in Northern Hemisphere conifers. *N. Phytol.* 216, 728–740. <https://doi.org/10.1111/nph.14639>.
- Björklund, J., von Arx, G., Nievergelt, D., Wilson, R., Van den Bulcke, J., Günther, B., Loader, N.J., Rydval, M., Fonti, P., Scharnweber, T., Andreu-Hayles, L., Büntgen, U., D'Arrigo, R., Davi, N., De Mil, T., Esper, J., Gärtner, H., Geary, J., Gunnarson, B.E., Hartl, C., Hevia, A., Song, H., Janecka, K., Kaczka, R.J., Kiryanov, A.V., Kochbeck, M., Liu, Y., Meko, M., Mundo, I., Nicolussi, K., Oelkers, R., Pichler, T., Sánchez-Salguero, R., Schneider, L., Schweingruber, F., Timonen, M., Trouet, V., Van Acker, J., Verstege, A., Villalba, R., Wilmking, M., Frank, D., 2019. Scientific merits and analytical challenges of tree-ring densitometry. *Rev. Geophys.* 57, 1224–1264. <https://doi.org/10.1029/2019rg000642>.
- Bontemps, J.-D., Gelhaye, P., Nepveu, G., Hervé, J.-C., 2013. When tree rings behave like foam: moderate historical decrease in the mean ring density of common beech paralleling a strong historical growth increase. *Ann. For. Sci.* 70, 329–343. <https://doi.org/10.1007/s13595-013-0263-2>.
- Bouriaud, O., Bréda, N., Le Moguédec, G., Nepveu, G., 2004. Modelling variability of wood density in beech as affected by ring age, radial growth and climate. *Trees* 18, 264–276. <https://doi.org/10.1007/s00468-003-0303-x>.

- Briffa, K.R., Schweingruber, F.H., Jones, P.D., Osborn, T.J., Shiyatov, S.G., Vaganov, E. A., 1998. Reduced sensitivity of recent tree-growth to temperature at high northern latitudes. *Nature* 391, 678–682. <https://doi.org/10.1038/35596>.
- Bunn, A.G., 2008. A dendrochronology program library in R (dplR). *Dendrochronologia* 26, 115–124. <https://doi.org/10.1016/j.dendro.2008.01.002>.
- Bussotti, F., Feduccia, M., Iacopetti, G., Maggino, F., Pollastrini, M., Selvi, F., 2018. Linking forest diversity and tree health: preliminary insights from a large-scale survey in Italy. *For. Ecosyst.* 5. <https://doi.org/10.1186/s40663-018-0130-6>.
- Cailleret, M., Dakos, V., Jansen, S., Robert, E.M., Aakala, T., Amoroso, M.M., Antos, J.A., Bigler, C., Bugmann, H., Caccianaga, M., Camarero, J.-J., Cherubini, P., Coyea, M.R., Cufar, K., Das, A.J., Davi, H., Gea-Izquierdo, G., Gillner, S., Haavik, L.J., Hartmann, H., Hereš, A.-M., Hultine, K.R., Janda, P., Kane, J.M., Kharuk, V.I., Kitzberger, T., Klein, T., Levanic, T., Linares, J.-C., Lombardi, F., Mäkinen, H., Mészáros, I., Metsaranta, J.M., Oberhuber, W., Papadopoulos, A., Petritan, A.M., Rohner, B., Sangüesa-Barreda, G., Smith, J.M., Stan, A.B., Stojanovic, D.B., Suarez, M.-L., Svoboda, M., Trotsiuk, V., Villalba, R., Westwood, A.R., Wyckoff, P.H., Martínez-Vilalta, J., 2019. Early-warning signals of individual tree mortality based on annual radial growth. *Front. Plant Sci.* 9. <https://doi.org/10.3389/fpls.2018.01964>.
- Carnicer, J., Coll, M., Ninyerola, M., Pons, X., Sanchez, G., Penuelas, J., 2011. Widespread crown condition decline, food web disruption, and amplified tree mortality with increased climate change-type drought. *Proceedings of the National Academy of Sciences* 108, 1474–1478. doi:10.1073/pnas.1010070108.
- Cherubini, P., Battipaglia, G., Innes, J.L., 2021. Tree vitality and forest health: can tree-ring stable isotopes be used as indicators. *Curr. For. Rep.* 7, 69–80. <https://doi.org/10.1007/s40725-021-00137-8>.
- Cufar, K., Prislan, P., De Luis, M., Gričar, J., 2008. Tree-ring variation, wood formation and phenology of beech (*Fagus sylvatica*) from a representative site in Slovenia, SE Central Europe. *Trees* 22, 749–758. <https://doi.org/10.1007/s00468-008-0235-6>.
- Davies, D., Loader, N.J., 2020. An evaluation of English oak earlywood vessel area as a climate proxy in the UK. *Dendrochronologia* 64, 125777. <https://doi.org/10.1016/j.dendro.2020.125777>.
- De Mil, T., Vannoppen, A., Beeckman, H., Van Acker, J., Van den Bulcke, J., 2016. A field-to-desktop toolchain for X-ray CT densitometry enables tree ring analysis. *Ann. Bot.* 117, 1187–1196. <https://doi.org/10.1093/aob/mcw063>.
- De Mil, T., Meko, M., Belmecheri, S., February, E., Therrell, M., Van den Bulcke, J., Trouet, V., 2021. A lonely dot on the map: Exploring the climate signal in tree-ring density and stable isotopes of clonal willow cedar, South Africa. *Dendrochronologia* 69, 125879. <https://doi.org/10.1016/j.dendro.2021.125879>.
- Debel, A., Meier, W.J.-H., Bräuning, A., 2021. Climate signals for growth variations of *F. sylvatica*, *P. abies*, and *P. sylvestris* in southeast Germany over the past 50 years. *Forests* 12, 1433. <https://doi.org/10.3390/f12111433>.
- Diaconu, D., Wassenberg, M., Spiecker, H., 2016. Variability of European beech wood density as influenced by interactions between tree-ring growth and aspect. *For. Ecosyst.* 3. <https://doi.org/10.1186/s40663-016-0065-8>.
- Dierick, M., Van Loo, D., Masschaele, B., Van den Bulcke, J., Van Acker, J., Cnudde, V., Van Hoorebeke, L., 2014. Recent micro-CT scanner developments at UGCT. *Nucl. Instrum. Methods Phys. Res. Sect. B: Beam Interact. Mater. At.* 324, 35–40. <https://doi.org/10.1016/j.nimb.2013.10.051>.
- Dittmar, C., Zech, W., Elling, W., 2003. Growth variations of Common beech (*Fagus sylvatica* L.) under different climatic and environmental conditions in Europe—a dendroecological study. *For. Ecol. Manag.* 173, 63–78. [https://doi.org/10.1016/s0378-1127\(01\)00816-7](https://doi.org/10.1016/s0378-1127(01)00816-7).
- Dorado-Liñán, I., Akhmetzyanov, L., Menzel, A., 2017. Climate threats on growth of near-edge European beech peripheral populations in Spain. *Int. J. Biometeorol.* 61, 2097–2110. <https://doi.org/10.1007/s00484-017-1410-5>.
- Esper, S., George, S., Anchukaitis, K., Darrigo, R., Ljungqvist, F.C., Luterbacher, J., Schneider, L., Stoffel, M., Wilson, R., Büntgen, U., 2018. Large-scale, millennial-length temperature reconstructions from tree-rings. *Dendrochronologia* 50, 81–90. <https://doi.org/10.1016/j.dendro.2018.06.001>.
- FOREST EUROPE, 2020. State of Europe's forests 2020.
- Fowler, A., Boswijk, G., 2003. Chronology stripping as a tool for enhancing the statistical quality of tree-ring chronologies. *Tree-Ring Res.* 59, 53–62.
- Giagli, K., Gričar, J., Vavřík, H., Menšík, L., Gryc, V., 2016. The effects of drought on wood formation in *Fagus sylvatica* during two contrasting years. *IAWA J.* 37, 332–348. <https://doi.org/10.1163/22941932-20160137>.
- Goossens, W., 2021. Wateropname via de bladeren bij beuk: een overlevingsstrategie tijdens droogte? *Bosrevue* 92a, 1–8.
- Gottardini, E., Cristofolini, F., Cristofori, A., Pollastrini, M., Camin, F., Ferretti, M., 2020. A multi-proxy approach reveals common and species-specific features associated with tree defoliation in broadleaved species. *For. Ecol. Manag.* 467, 118151. <https://doi.org/10.1016/j.foreco.2020.118151>.
- Hanewinkel, M., Cullmann, D.A., Schelhaas, M.-J., Nabuurs, G.-J., Zimmermann, N.E., 2013. Climate change may cause severe loss in the economic value of European forest land. *Nat. Clim. Change* 3, 203–207. <https://doi.org/10.1038/nclimate1687>.
- Hartmann, H., Moura, C.F., Anderegg, W.R., Ruehr, N.K., Salmon, Y., Allen, C.D., Arndt, S.K., Breshears, D.D., Davi, H., Galbraith, D., Ruthrof, K.X., Wunder, J., Adams, H.D., Bloemen, J., Cailleret, M., Cobb, R., Gessler, A., Grams, T.E., Jansen, S., Kautz, M., Lloret, F., O'Brien, M., 2018. Research frontiers for improving our understanding of drought-induced tree and forest mortality. *N. Phytol.* 218, 15–28. <https://doi.org/10.1111/nph.15048>.
- Jacquin, P., Longuetaud, F., Leban, J.-M., Mothe, F., 2017. X-ray microdensitometry of wood: A review of existing principles and Devices. *Dendrochronologia* 42, 42–50. <https://doi.org/10.1016/j.dendro.2017.01.004>.
- Jevšenak, J., 2020. New features in the dendroTools R package: Bootstrapped and partial correlation coefficients for monthly and daily climate data. *Dendrochronologia* 63, 125753. <https://doi.org/10.1016/j.dendro.2020.125753>.
- Jevšenak, J., Levanič, T., 2018. dendroTools: R package for studying linear and nonlinear responses between tree-rings and daily environmental data. *Dendrochronologia* 48, 32–39. <https://doi.org/10.1016/j.dendro.2018.01.005>.
- Klippel, L., Krusic, P.J., Konter, S., O., George, S., Trouet, V., Esper, J., 2019. A 1200 year reconstruction of temperature extremes for the northeastern Mediterranean region. *Int. J. Climatol.* 39, 2336–2350. <https://doi.org/10.1002/joc.5955>.
- Kozłowski, T.T., Pallardy, S.G., 1997. Growth Control in Woody Plants. Acad. Press, San Diego, CA.
- Lebourgeois, F., Bréda, N., Ulrich, E., Granier, A., 2005. Climate-tree-growth relationships of European beech (*Fagus sylvatica* L.) in the French Permanent Plot. *Netw. (RENECOFOR). Trees* 19, 385–401. <https://doi.org/10.1007/s00468-004-0397-9>.
- Lehnebach, R., Campioli, M., Gričar, J., Prislan, P., Mariën, B., Beeckman, H., Van den Bulcke, J., 2021. High-resolution X-ray computed tomography: a new workflow for the analysis of xylogenesis and intra-seasonal wood biomass production. *Front. Plant Sci.* 12. <https://doi.org/10.3389/fpls.2021.698640>.
- van der Maaten, E., van der Maaten-Theunissen, M., Spiecker, H., 2012. Temporally resolved intra-annual wood density variations in European beech (*Fagus sylvatica* L.) as affected by climate and aspect. *Ann. For. Res.* 55 (1), 113–124.
- Maes, S.L., Vannoppen, A., Altman, J., Van den Bulcke, J., Decocq, G., De Mil, T., Depauw, L., Landuyt, D., Perring, M.P., Van Acker, J., Vanhellemont, M., Verheyen, K., 2017. Evaluating the robustness of three ring-width measurement methods for growth release reconstruction. *Dendrochronologia* 46, 67–76. <https://doi.org/10.1016/j.dendro.2017.10.005>.
- Massart, L., 2017. Does *Quercus rubra* recover faster after drought stress in mixed forests? PhD thesis, Ghent University.
- McDowell, N., Pockman, W.T., Allen, C.D., Breshears, D.D., Cobb, N., Kolb, T., Plaut, J., Sperry, J., West, A., Williams, D.G., Yepez, E.A., 2008. Mechanisms of plant survival and mortality during drought: why do some plants survive while others succumb to drought. *N. Phytol.* 178, 719–739. <https://doi.org/10.1111/j.1469-8137.2008.02436.x>.
- Meinardus, C., Bayer, E., Lasermann, B., Singer, A., Bräuning, A., 2012. Reactions and recovery times of *Fagus sylvatica* after drought events derived from ring width and maximum latewood density. *DENDROSYMPOSIUM* 2011 93.
- Meyer, B.F., Buras, A., Rammig, A., Zang, C.S., 2020. Higher susceptibility of beech to drought in comparison to oak. *Dendrochronologia* 64, 125780. <https://doi.org/10.1016/j.dendro.2020.125780>.
- Michelot, A., Simard, S., Rathgeber, C., Dufrene, E., Damesin, C., 2012. Comparing the intra-annual wood formation of three European species (*Fagus sylvatica*, *Quercus petraea* and *Pinus sylvestris*) as related to leaf phenology and non-structural carbohydrate dynamics. *Tree Physiol.* 32, 1033–1045. <https://doi.org/10.1093/treephys/tps052>.
- Miranda, J.C., Calderaro, C., Coccozza, C., Lasserre, B., Tognetti, R., von Arx, G., 2022. Wood anatomical responses of European beech to elevation, land use change, and climate variability in the central Apennines, Italy. *Front. Plant Sci.* 13. doi:10.3389/fpls.2022.855741.
- Peters, R., von Arx, G., Nievergelt, D., Ibrom, A., Stillhard, J., Trotsiuk, V., Mazurkiewicz, A., Babst, F., 2020. Axial changes in wood functional traits have limited net effects on stem biomass increment in European beech (*Fagus sylvatica*). *Tree Physiology* 40 (4), 498–510. <https://doi.org/10.1093/treephys/tpaa002>.
- Prislan, P., Gričar, J., De Luis, M., Smith, K.T., Cufar, K., 2013. Phenological variation in xylem and phloem formation in *Fagus sylvatica* from two contrasting sites. *Agric. For. Meteorol.* 180, 142–151. <https://doi.org/10.1016/j.agrformet.2013.06.001>.
- Pritzkow, C., Wazny, T., Heußner, K., Słowiński, M., Bieber, A., Liñán, I.D., Helle, G., Heinrich, I., 2016. Minimum winter temperature reconstruction from average earlywood vessel area of European oak (*Quercus robur*) in N-Poland. *Palaeogeogr., Palaeoclimatol., Palaeoecol.* 449, 520–530. <https://doi.org/10.1016/j.palaeo.2016.02.046>.
- Puchi, P.F., Castagneri, D., Rossi, S., Carrer, M., 2020. Wood anatomical traits in black spruce reveal latent water constraints on the boreal forest. *Glob. Change Biol.* 26, 1767–1777. <https://doi.org/10.1111/gcb.14906>.
- R Core Team, 2021. R: A language and environment for statistical computing. R Foundation for Statistical Computing, Vienna, Austria. URL (<https://www.R-project.org/>).
- Reyer, C.P., Leuzinger, S., Rammig, A., Wolf, A., Bartholomeus, R.P., Bonfante, A., de Lorenzi, F., Dury, M., Gloning, P., Jaoudé, R.A., Klein, T., Kuster, T.M., Martins, M., Niedrist, G., Riccardi, M., Wohlfahrt, G., De Angelis, P., De Dato, G., François, L., Menzel, A., Pereira, M., 2013. A plants perspective of extremes: terrestrial plant responses to changing climatic variability. *Glob. Change Biol.* 19, 75–89. <https://doi.org/10.1111/gcb.12023>.
- del Río, M., Pretzsch, H., Ruiz-Peinado, R., Ampoorter, E., Annighöfer, P., Barbeito, I., Bielak, K., Brazaitis, G., Coll, L., Drössler, L., Fabrika, M., Forrester, D.I., Heym, M., Hurt, V., Kurylyak, V., Löf, M., Lombardi, F., Madrickiene, E., Matović, B., Mohren, F., Motta, R., Ouden, J., Pach, M., Ponette, Q., Schütz, G., Skrzyszewski, J., Sramek, V., Sterba, H., Stojanović, D., Svoboda, M., Zlatanov, T.M., Bravo-Oviedo, A., 2017. Species interactions increase the temporal stability of community productivity in *Pinus sylvestris*-*Fagus sylvatica* mixtures across Europe. *J. Ecol.* 105, 1032–1043. <https://doi.org/10.1111/1365-2745.12727>.
- Schneider, C.A., Rasband, W.S., Eliceiri, K.W., 2012. NIH image to imagej: 25 years of image analysis. *Nat. Methods* 9, 671–675. <https://doi.org/10.1038/nmeth.2089>.
- Scholze, M., Knorr, W., Arnell, N.W., Prentice, I.C., 2006. A climate-change risk analysis for world ecosystems. *Proceedings of the National Academy of Sciences* 103, 13116–13120. doi:10.1073/pnas.0601816103.

- Schweingruber, F., Fritts, H., Bräker, O., Drew, L., Schär, E., 1978. The X-ray technique as applied to dendroclimatology.
- Skomarkova, M.V., Vaganov, E.A., Mund, M., Knohl, A., Linke, P., Boerner, A., Schulze, E.-D., 2006. Inter-annual and seasonal variability of radial growth, wood density and carbon isotope ratios in tree rings of beech (*Fagus sylvatica*) growing in Germany and Italy. *Trees* 20, 571–586. <https://doi.org/10.1007/s00468-006-0072-4>.
- Sousa-Silva, R., Verheyen, K., Ponette, Q., Bay, E., Sioen, G., Titeux, H., Van De Peer, T., Van Meerbeek, K., Muys, B., 2018. Tree diversity mitigates defoliation after a drought-induced tipping point. *Glob. Change Biol.* 24, 4304–4315. <https://doi.org/10.1111/gcb.14326>.
- St. George, S., Esper, J., 2019. Concord and discord among Northern Hemisphere paleotemperature reconstructions from tree rings. *Quat. Sci. Rev.* 203, 278–281. <https://doi.org/10.1016/j.quascirev.2018.11.013>.
- Trouet, V., Van Oldenborgh, G.J., 2013. KNMI Climate Explorer: a web-based research tool for high-resolution paleoclimatology. *Tree-Ring Res.* 69, 3–13. <https://doi.org/10.3959/1536-1098-69.1.3>.
- Vaganov, E.A., Hughes, M.K., Shashkin, A.V., 2006. *Growth Dynamics of Conifer Tree Rings: Images of Past and Future Environments*. Springer, Berlin.
- Van den Bulcke, J., Wernersson, E.L., Dierick, M., Van Loo, D., Masschaele, B., Brabant, L., Boone, M.N., Van Hoorebeke, L., Haneca, K., Brun, A., Hendriks, C.L.L., Van Acker, J., 2014. 3D tree-ring analysis using helical X-ray tomography. *Dendrochronologia* 32, 39–46. <https://doi.org/10.1016/j.dendro.2013.07.001>.
- Van den Bulcke, J., Boone, M.A., Dhaene, J., Van Loo, D., Van Hoorebeke, L., Boone, M. N., Wyffels, F., Beeckman, H., Van Acker, J., De Mil, T., 2019. Advanced X-ray CT scanning can boost tree ring research for earth system sciences. *Ann. Bot.* 124, 837–847. <https://doi.org/10.1093/aob/mcz126>.
- Van Der Werf, G., Sass-Klaassen, U.G., Mohren, G., 2007. The impact of the 2003 summer drought on the intra-annual growth pattern of beech (*Fagus sylvatica* L.) and oak (*Quercus robur* L.) on a dry site in the Netherlands. *Dendrochronologia* 25, 103–112. <https://doi.org/10.1016/j.dendro.2007.03.004>.
- Vanhellemont, M., Sousa-Silva, R., Maes, S.L., Van den Bulcke, J., Hertzog, L., De Groote, S., Van Acker, J., Bonte, D., Martel, A., Lens, L., Verheyen, K., 2019. Distinct growth responses to drought for oak and beech in temperate mixed forests. *Sci. Total Environ.* 650, 3017–3026. <https://doi.org/10.1016/j.scitotenv.2018.10.054>.
- Vannoppen, A., Maes, S., Kint, V., De Mil, T., Ponette, Q., Van Acker, J., Van den Bulcke, J., Verheyen, K., Muys, B., 2017. Using X-ray CT based tree-ring width data for tree growth trend analysis. *Dendrochronologia* 44, 66–75. <https://doi.org/10.1016/j.dendro.2017.03.003>.
- Vicente-Serrano, S.M., Beguería, S., López-Moreno, J.I., 2010. A multiscalar drought index sensitive to global warming: the standardized precipitation evapotranspiration index. *J. Clim.* 23, 1696–1718. <https://doi.org/10.1175/2009jcli2909.1>.
- Vlassenbroeck, J., Masschaele, B., Dierick, M., Cnudde, V., De Witte, Y., Pieters, K., Van Hoorebeke, L., Jacobs, P., 2007. Recent developments in the field of X-ray nano- and micro-CT at the Centre for X-ray Tomography of the Ghent University. *Microsc. Microanal.* 13. <https://doi.org/10.1017/s1431927607077379>.
- von Arx, G., Kueffer, C., Fonti, P., 2013. Quantifying plasticity in vessel grouping – added value from the image analysis tool ROXAS. *IAWA J.* 34, 433–445. <https://doi.org/10.1163/22941932-00000035>.
- Von Arx, R.L., Nievergelt, G., Ibrom, D., Stillhard, A., Trotsiuk, J., Mazurkiewicz, V., Babst, F.A., 2020. Axial changes in wood functional traits have limited net effects on stem biomass increment in European beech (*Fagus sylvatica*). *Tree Physiol.* 40, 498–510. <https://doi.org/10.1093/treephys/tpaa002>.
- Z'Graggen, S., 1992. *Dendrohistometrische-klimatologische Untersuchung an Buchen (Fagus sylvatica L.)*. Diss., Univ. Basel, Basel 167.
- Zang, C., Biondi, F., 2015. Treeclim: An R package for the numerical calibration of proxy-climate relationships. *Ecography* 38, 431–436. <https://doi.org/10.1111/ecog.01335>.
- Zhang, S.Y., 1995. Effect of growth rate on wood specific gravity and selected mechanical properties in individual species from distinct wood categories. *Wood Sci. Technol.* 29. <https://doi.org/10.1007/bf00194204>.